

A Further Note on Båth's Law

David Vere-Jones¹, Junko Murakami² and Annemarie Christophersen²

¹ Victoria University and Statistical Research Associates, Wellington, New Zealand

² Victoria University, Wellington, New Zealand

Corresponding author: dvj@mcs.vuw.ac.nz

AIM: To show how Båth's law arises in an elementary aftershock model

I. Model Assumptions and Basic Model Properties

(a) The magnitudes of successive events in a sequence are distributed identically and independently (independently also of the number $N(M^*)$ in the sequence) with common distribution

$$1 - F(M) = \Pr\{Mag > M\} = e^{-\beta(M-M_0)} = 10^{-b(M-M_0)}; \quad (1)$$

$$\beta \approx 2.30b.$$

(Notes: M_0 here is a scaling origin, commonly but not necessarily related to catalogue completeness. For mathematical convenience, in the rest of the poster we use logarithms to base e rather than to base 10, hence β rather than b .)

(b) The aftershock structure is determined by the magnitude of the initiating event. In particular, the expected number $E[N(M^*)] \equiv \mu(M^*)$ of events above the threshold M_0 , and generated by an initiating event of magnitude M^* , is assumed to satisfy the scaling relation

$$\mu(M^*) = Ae^{\alpha(M^*-M_0)}, \quad (2)$$

Figure 1(a) compares (2) with the empirical results from the California data, as described in Section IV, with $\alpha = \beta$ and $b = 0.91$ from Reasenberg and Jones (1989).

(c) It follows that the expected number of events above some intermediate threshold M_c , given an initiating event of size M^* , is given by

$$\mu(M_c | M^*) = p\mu(M^*) = e^{-\beta(M_c-M_0)} Ae^{\alpha(M^*-M_0)}, \quad (3)$$

since each of the initial events has the same probability $p = e^{-\beta(M_c-M_0)}$ of reaching the threshold M_c .

(d) The expected number of events larger than the initiating event is thus given by

$$\rho(M^*) \equiv \mu(M^* | M^*) = Ae^{(\alpha-\beta)(M^*-M_0)}. \quad (4)$$

If $\alpha > \beta$ the system is essentially unstable since the larger the event the more likely it is to produce an even larger aftershock. Thus interest centres on systems with $\alpha \leq \beta$, and particularly with the case $\alpha = \beta$, which corresponds to the critical case in branching models and is associated with self-similarity.

(e) If the right side of (4) is small enough (say below 10%), then

$$\Pr\{\text{largest aftershock} \geq M^*\} \approx \rho(M^*) = Ae^{(\alpha-\beta)(M^*-M_0)}. \quad (5)$$

The left side here can be interpreted as *the probability that the initiating event is a foreshock*. If $\alpha = \beta$, this probability is independent of the magnitude of the initiating event: $\rho(M^*) \approx A$. Results from the California data are shown in Figure 1(c) and compared with the proportion .05.

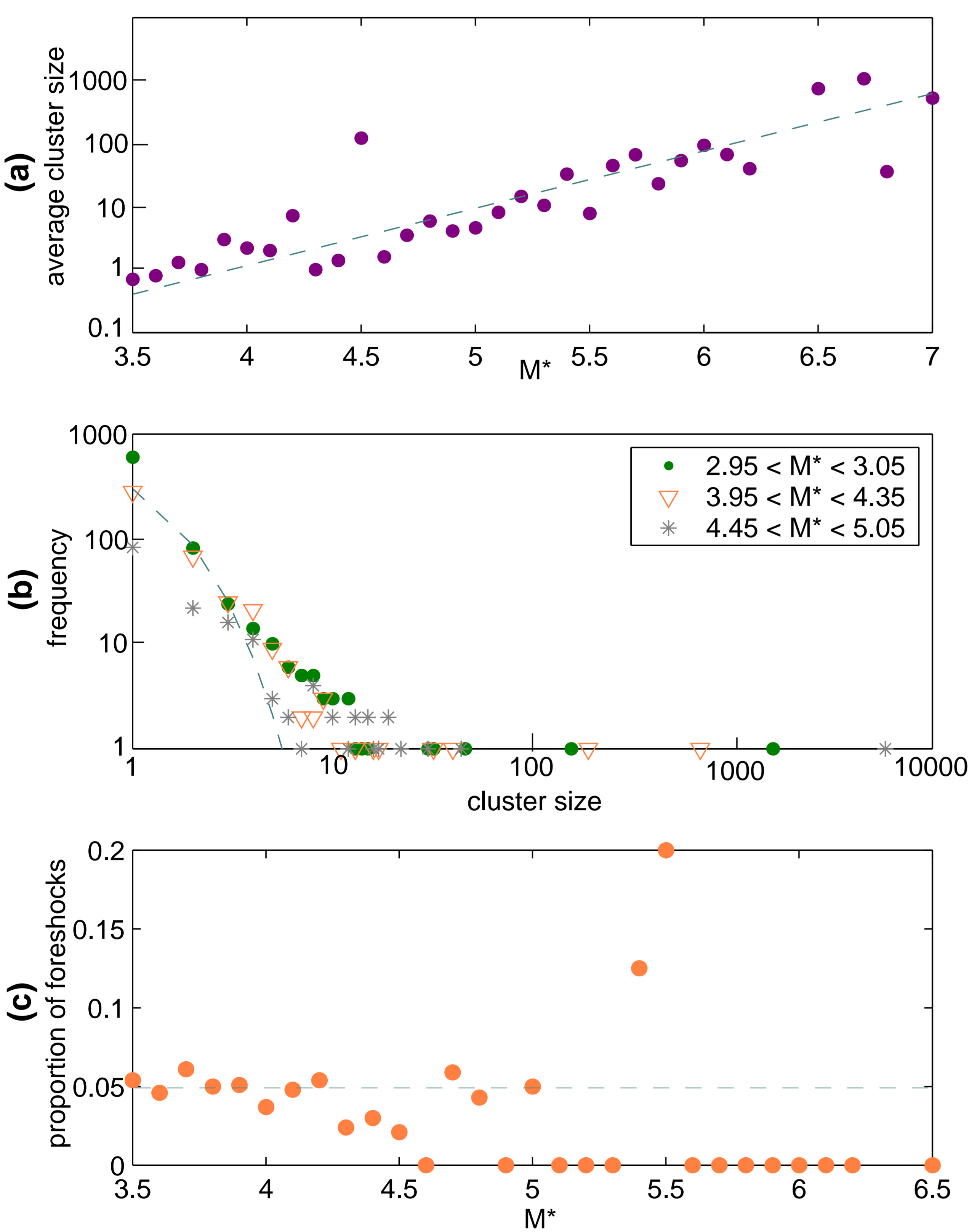


Figure 1: (a) The cluster size (in log base 10), excluding the initial event, plotted against M^* together with the line $\log_{10}(A) + b(M^* - 2.5)$, where $A = 0.05$ and $b = 0.91$. (b) The frequency of cluster sizes; the line is for a geometric distribution. (c) The proportion of initiating events that are foreshocks.

II. Expected value of the magnitude of the largest aftershock

(a) Now let M_{max} denote the magnitude of the largest event in the sequence (excluding the initiating event). For given N , the distribution of $M_{max} - M_0$ is given by

$$F_{max}(M | N) = \Pr\{M_{max} - M_0 \leq M | N\} = [1 - e^{-\beta(M-M_0)}]^N. \quad (6)$$

(b) This has mode $(1/\beta) \log N$ and mean

$$E[M_{max} - M_0 | N] = \frac{1}{\beta} \left[1 + \frac{1}{2} + \frac{1}{3} + \dots + \frac{1}{N-1} \right] \approx \frac{1}{\beta} (\log N + \gamma) \quad (7)$$

where $\gamma \approx .577$ is Euler's constant.

(c) Taking expectations over N , using the first order approximation $E[\log N] \approx \log[E(N)]$, and substituting from (2) we obtain

$$E[M_{max} - M_0] \approx \frac{1}{\beta} \log[\mu(M^*)] = \frac{\alpha}{\beta} (M^* - M_0) + \frac{\log A}{\beta}, \quad (8)$$

whence

$$E[M^* - M_{max}] = \frac{\beta - \alpha}{\beta} (M^* - M_0) - \frac{1}{\beta} \log A = \frac{1}{\beta} \log \rho(M^*). \quad (9)$$

This equation reflects Utsu's (1961) empirical law for the Båth's law discrepancy.

(d) Equations (5) and (9) link the *foreshock probability* to the expected discrepancy in Båth's law. Taking $A = .05$ as a representative value of the former, and assuming $\alpha = \beta$, the model predicts an average Båth's law discrepancy of about $3/2.3 \approx 1.3$.

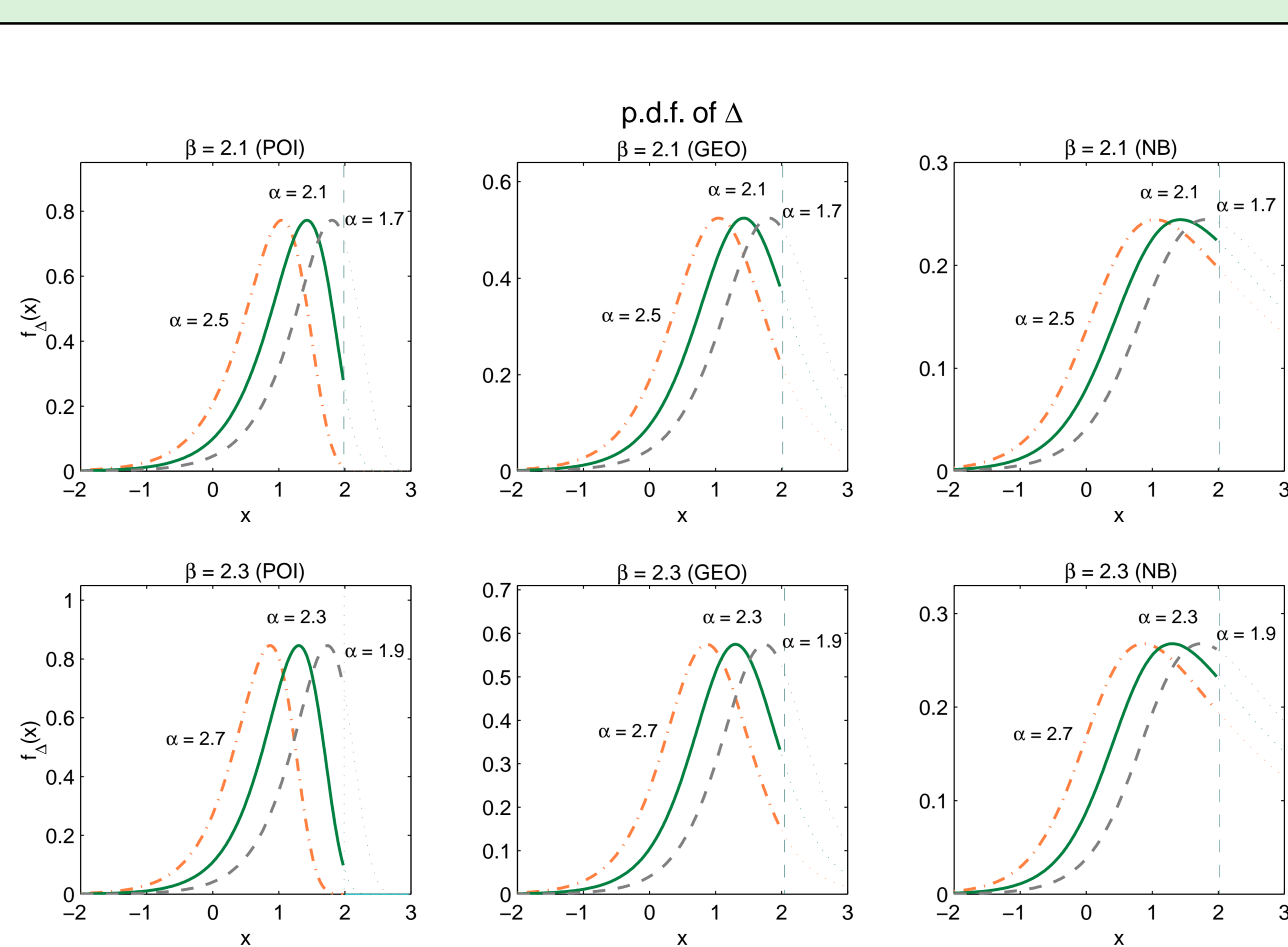


Figure 2: The p.d.f. of $\Delta = M^* - M_{max}$ with $N(M^*) \sim POI(\lambda)$, $GEO(p)$, and $NB(K, \bar{p})$, where $M^* = 4.5$, $M_0 = 2.5$, and $A = .05$, so that $\mu(4.5) = Ae^{2\alpha} = \lambda = \frac{1-p}{p} = K \frac{1-p}{p}$. The top three graphs correspond to $\beta = 2.1$, $\alpha = 1.7, 2.1, 2.5$, the bottom three to $\beta = 2.3$, $\alpha = 1.9, 2.3, 2.7$.

III. Distribution of the magnitude of the largest aftershock

(a) Let $G_{M^*}(z) = E(z^N)$ be the probability generating function (p.g.f.) of the number $N = N(M^*)$ of aftershock events with $M > M_0$, initiated by an event of magnitude M^* . Taking expectations over N in (6), and setting $M_{max} = M_0$ if $N = 0$, leads to

$$F_{max}(M) = G_{M^*}[1 - e^{-\beta(M-M_0)}]. \quad (10)$$

(b) Hence, if $\Delta = M^* - M_{max}$,

$$1 - F_{\Delta}(x) = \Pr(\Delta \geq x) = \Pr(M_{max} \leq M^* - x) = G_{M^*}[1 - e^{-\beta(M^*-M_0-x)}]. \quad (11)$$

Here negative values of x correspond to cases where the initiating event acts as a foreshock. Positive values of x are restricted to the region $x \leq M^* - M_0$, as illustrated by the vertical bars in the Figure 2.

(c) Specific examples can now be studied by selecting particular forms for the distribution of $N(M^*)$. Figure 2 shows probability densities for Δ for three choices of the distribution of $N(M^*)$ – Poisson, geometric, and negative binomial with shape parameter $K = 0.2$ – and various values of α and β . The empirical number distribution is shown in Figure 1(b).

(d) All graphs show a peak at close to 1.3, the value suggested by the link to the foreshock probability referred to earlier. The width of the peak (and hence the effect of the truncation), varies according to the tail of the number distribution. It is much broader in the third example, which has the longest tail.

(e) Empirical results are shown for the California data in Figure 3, using a 3-point moving average.

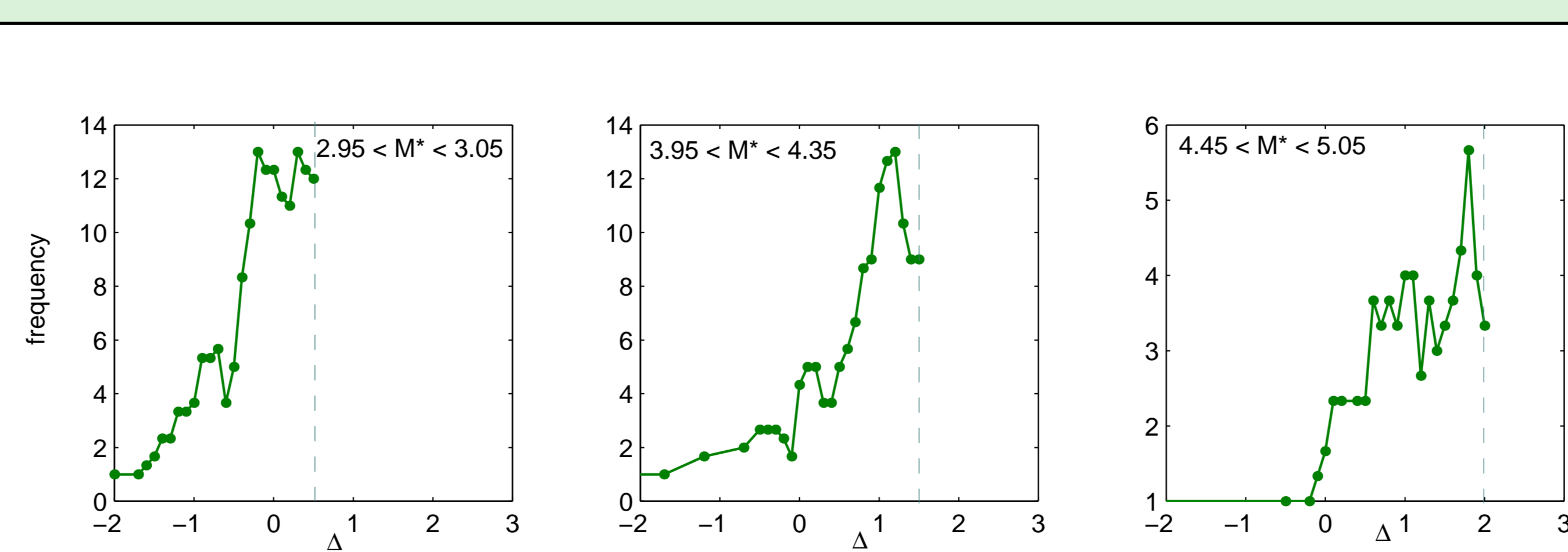


Figure 3: The frequency distribution of Δ for various M^* , obtained from the California data. The graphs include the magnitude differences of doublets which could not be fitted by ellipses.

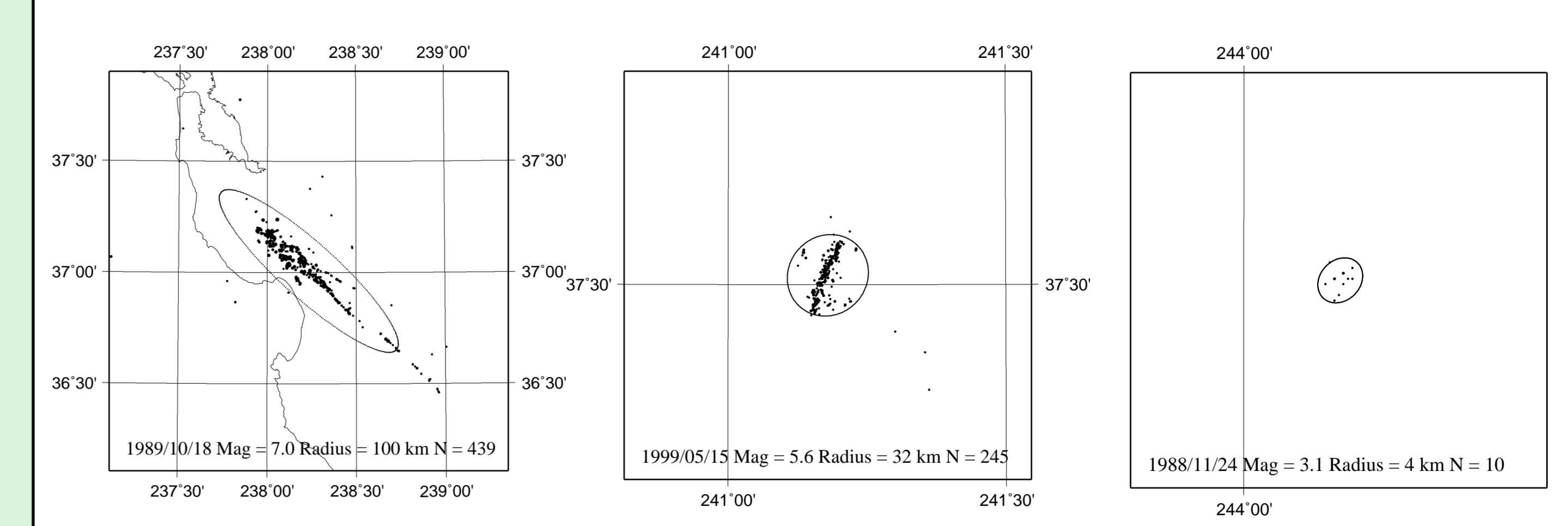


Figure 4: Three examples of the ellipse fitting. Each map is centred on the mean of the epicentre distribution. The width of each map corresponds to twice the search radius of the mainshock as given in the caption of each figure.

IV. Comparison with the California Data

Although the model is crude, it can be put into rough comparison with empirical data provided one can find objective and consistent definitions of an 'initiating event' and a 'sequence'. For this purpose we used the methodology developed by Christophersen (2000), as outlined briefly below, on California data from the ANSS (Advanced National Seismic Systems) for 1984–2004 between latitude 31–43 North and longitude 127–112 East. Data were restricted to events with depths shallower than 40 km and magnitudes above 2.49.

We defined earthquake clusters via a two step process. First the catalogue was searched for sequences containing at least one earthquake above a minimum magnitude (3 was chosen in the examples illustrated). Events considered as possibly belonging to the sequence associated with any one such earthquake were required to lie within a radial distance from the largest event in the sequence, following Uhrhammer (2005); radii of 4 km, 9km, 20km, 45km to 92 km were used to define regions associated with earthquakes of magnitude, 3, 4, 5, 6, and 7 respectively. A time delay of at most 10 days from the previous most recent event associated with the sequence was used to determine the duration of the sequence.

Each initial sequence with at least 3 earthquakes was then fitted by an ellipse using the scatter of the epicentres (for more details see Christophersen, 2000). Figure 4 shows three examples illustrating three different magnitudes for the initiating event. The first event in time that occurred within the ellipse was defined as the initiating earthquake for the purposes of the previous analysis. We calculated the magnitude difference between the initiating event and the largest earthquake within the ellipse, or the second largest if the largest earthquake occurred first.

V. Discussion

Despite the simplicity of the model, there are good qualitative and even quantitative agreements between the predictions of the model and the empirical data. The most obvious discrepancies relate to the distribution of the numbers of events for an initiating event of given magnitude. The real data include complex sequences with several stages or branching episodes, which are not well captured within this simple model framework. However, the broad agreement with the scaling relation (4), the near constancy of the foreshock probability (9), and, perhaps less convincingly, the shape of the Båth's law discrepancy Δ , all suggest that switching the focus of the discussion from the magnitude of the largest event in the sequence, to the magnitude of the initiating event has some basis in the physical reality which the model is trying to capture.

Overall, the model and analysis provide support for the idea that Båth's law does not have a separate physical cause, but is rather a consequence of basic scaling relationships for the magnitudes of the earthquakes and the events related to them. Some further discussions of this issue are listed in the references.

Acknowledgements

We are grateful to Didier Sornette, Rudolfo Console and Jiancang Zhuang for comments on an initial draft of this poster. The work was partially supported by grants from the New Zealand Earthquake Commission and the New Zealand Institute of Mathematics and Its Applications. The authors gratefully acknowledge the travel support from the conference organisers.

References

- Christophersen, A. (2000) The probability of a damaging earthquake following a damaging earthquake. Ph.D. Thesis, Victoria University of Wellington.
- Console, R., Lombardi, A.M., and Murru, M. (2003). Båth's law and the self-similarity of earthquakes. *Journal of Geophysical Research*, **108** N0 B2, 2128, doi: 10.1029/2001JB001651, 2003.
- Helmstetter, A. and Sornette, D. (2003) Båth's law derived from the Gutenberg-Richter law and from aftershock properties. *Geophysical Research Letters*, **30**, 2069, doi: 10.1029/2003GL018186.
- Lombardi, A.M. (2002) Probabilistic interpretation of Båth's law. *Ann. Geophysics* **45** 455-472.
- Reasenberg, P.A., and Jones, L.M. (1989) Earthquake hazard after a mainshock in California, *Science* **243** 1173-1176.
- Saichev, A. and Sornette, D. (2005) Distribution of the largest aftershocks in branching models of triggered seismicity: Theory of Båth's law. *Physical Review E* **71**, 056127
- Scherbakov, R. and Turcotte, D.L. (2004) A modified form of Båth's law. *Bulletin of the American Seismological Society* **94** 1968-1975.
- Uhrhammer, R. (2005) Personal communication.
- Utsu, T. (1961) A statistical study on the occurrence of aftershocks. *Geophysical Magazine* **30**, 521-605.
- Vere-Jones, D. (1969) A note on the statistical interpretation of Båth's law. *Bulletin of the American Seismological Society* **59** 1535-1541.
- Zhuang, J. and Ogata, Y. (2005) Properties of the probability distributions associated with the largest event in an earthquake cluster and their implications to foreshocks. (preprint)